

Electronic Supporting Information (ESI) for:

Atomically-Resolved Edge States on Surface-Nanotemplated Graphene Explored at Room Temperature

Pablo Merino^{1,+}, *Hernán Santos*², *Anna L. Pinardi*³, *Leonor Chico*³, *José A. Martín-Gago*^{1,3}

¹ *Centro de Astrobiología, INTA-CSIC, Carretera de Ajalvir km. 4, E-28850, Torrejón de Ardoz, Spain.*

² *Departamento de Física Fundamental, Universidad Nacional de Educación a Distancia, E-28040, Madrid, Spain*

³ *Instituto de Ciencia de Materiales de Madrid, CSIC, c/ Sor Juana Inés de la Cruz 3, E28049, Madrid, Spain.*

⁺ *Present address: Max Planck Institute for Solid State Research, Heisenbergstrasse 1, D-70569, Stuttgart, Germany.*

In this supplementary information we provide the total energy, band structure and spin characterization of wide GNR with (3,1) edge obtained from *ab-initio* calculations (1). We focus on the magnetization per atom, M , at the edges due to the edge-edge interaction $M=N_{\text{up}}-N_{\text{down}}$, where $N_{\text{up(down)}}$ is the number of electrons with spin up(down) per atom. (2) We checked that the total magnetization of the ribbons corresponds to the p_z orbitals by 95%.

Ab-initio calculations were performed with hydrogen saturation. In the energy window of experimental interest for this work, hydrogen saturation does not play any role, because the sigma bonds formed are completely well up or down in energy. This is why the π bands agree very satisfactorily with those obtained within the one-orbital tight-binding approximation.

For the evaluation of electronic and magnetic properties of (3,1) GNRs we use unit cells with several sizes, ranging from 60 atoms ($W=1.7$ nm) to 320 atoms ($W=10$ nm), up to the limit of our computational capacity. Fig. Supp. 1 and Fig. Supp. 2 show the band structure and magnetization of (3,1) ribbons for 1.7 nm and 10 nm widths,

respectively. In accordance with Ref (3) the number of zigzag atoms in the GNR (3,1) minimal unit is 2. Therefore, the calculated total energy difference per zigzag edge atom between spin-polarized and nonspin-polarized edge states is increased from 26 meV to 65 meV for widths from 1.7 nm to 10 nm, respectively, in good agreement with other calculations (4). This indicates the tendency of wide ribbons to be spin-polarized.

On the other hand, the total energy difference per zigzag edge atom between AFM and FM spin configurations is 13.5 meV ($W=1.7$ nm) and 0.35 meV ($W=10$ nm), indicating that the two configurations are almost equally stable for the wider ribbon. Moreover, the maximum magnetization of the edge atoms increases as the ribbon width increases ($M=0.16 \mu_B$ and $M=0.22 \mu_B$ for $W=1.7$ nm and $W=10$ nm, respectively). We interpret these results as a proof of magnetic decoupling between edge states for wide ribbons. Therefore, their magnetic behavior is as that of isolated magnetic edge states. Note that the atom resolved net spin-density appears around both edges and closely following the LDOS of the one-edge terminated graphene shown by the tight-binding calculations. We also point out the decrease of the gap energy in the AFM configuration with the width increase, varying from 0.39 eV for the thin GNR to 0.13 eV for the 10 nm GNR.

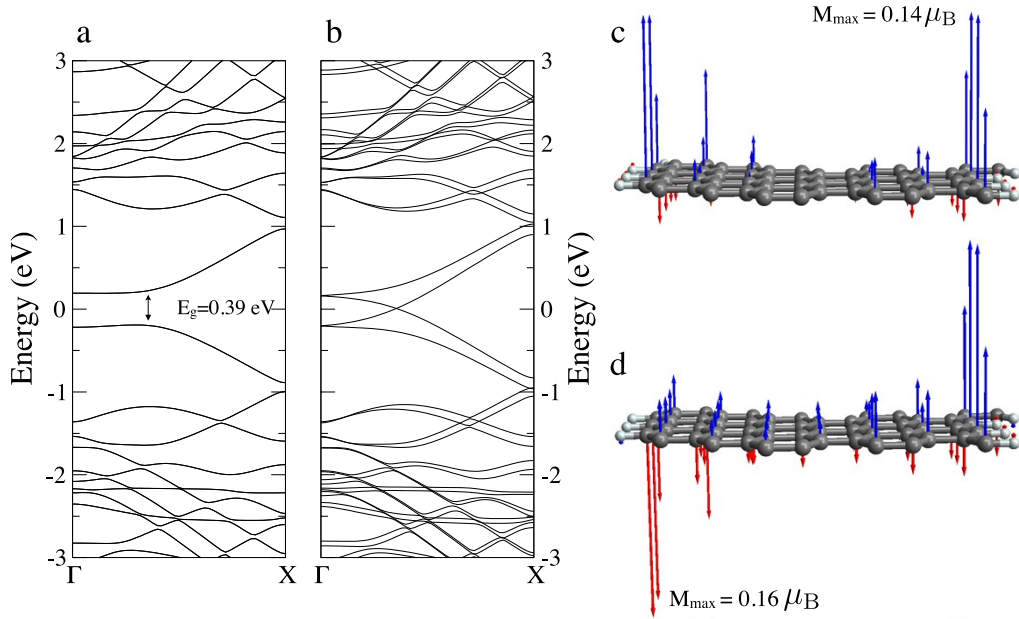


Figure Supp. 1: Band structure and magnetization per atom of the (3,1) GNR of 1.7 nm width. The AFM (FM) configuration is shown in (a) and (d) ((b) and (c)).

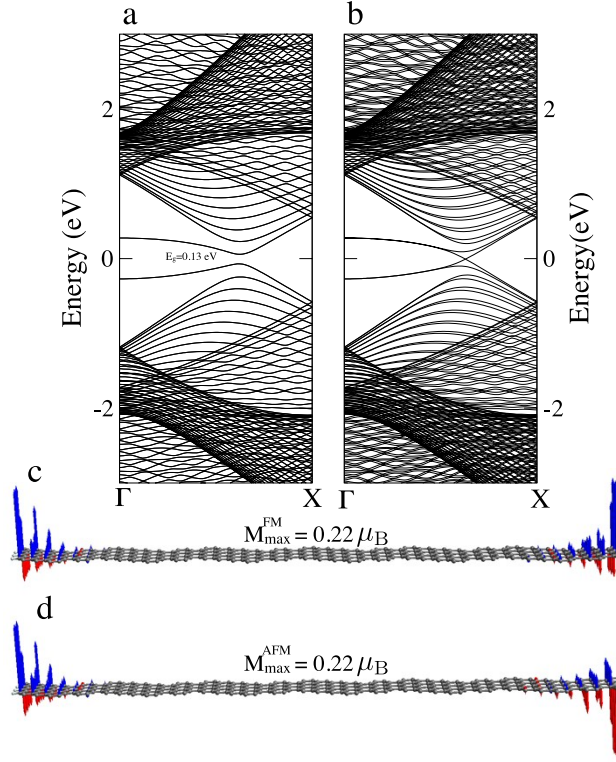


Figure Supp. 2: Band structure and magnetization per atom of the (3,1) GNR of 10 nm width. The AFM (FM) configuration is shown in (a) and (d) ((b) and (c)).

In addition, we provide the band dispersion and the spatially-resolved DOS of semi-infinite graphene sheets obtained with tight binding calculations. In particular, we present the armchair-terminated edge which does not present any edge state at the Fermi energy (Fig. Supp. 3 a), the zigzag terminated edge with one edge state at Fermi energy from $2/3 \Gamma X$ to X (Fig. Supp. 3 b, d) and the pure (3,1) edge that presents an edge state from Γ to $2/3 \Gamma X$ (see Figure Supp. 3 c, e).

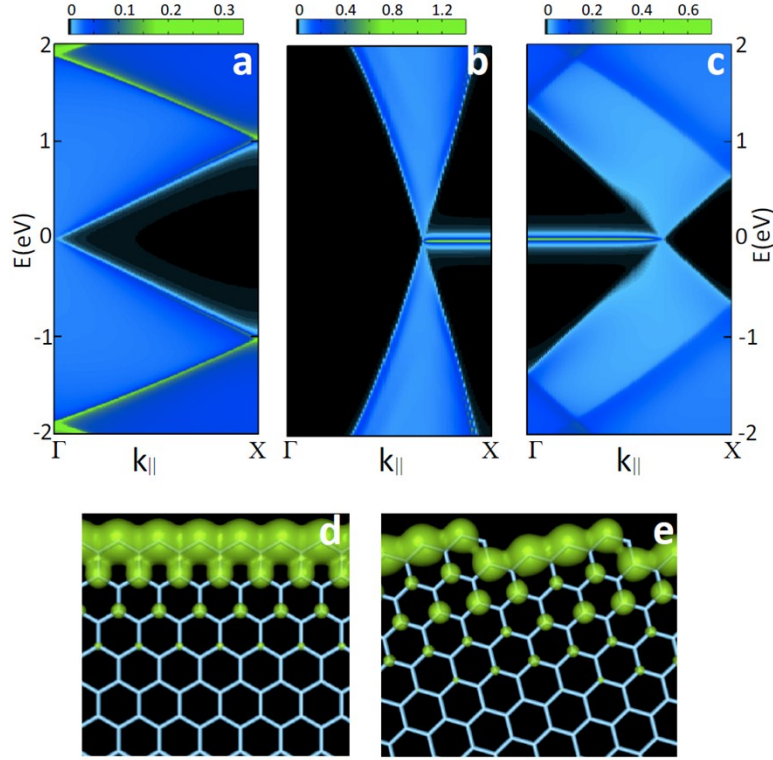


Figure Supp. 3: Band dispersion of armchair (a), zigzag (b) and pure (3,1) (c) semi-infinite graphene. The real weight of DOS at Fermi level of zigzag and pure (3,1) semi-infinite is represented in (d) and (e), respectively.

We provide data with minimal processing (only partial plane was applied to topographic images to remove the overall tilt) to preclude any possible effect of feedback in the current error maps presented in Fig. 2 of the main manuscript. All images were obtained descending the tip from upper terraces to lower terraces. Nevertheless the feedback loop forces the tip to perform a strong movement upwards prior descending the Pt step. Feedback circuits compare the output of the current amplifier with a reference voltage which represents the setpoint of the tunneling current. The error signal is sent to the feedback circuit, which sends a voltage to the z piezo: if the tunneling current is larger than the preset current, then the voltage applied to the z piezo tends to withdraw the tip from the sample surface and vice versa.⁵ Given the scan direction the only possible effect of feedback loop settings would be a broadening of the appearance of the lower step; never a sudden retraction of the tip. Additionally, Fig. 4 of the main manuscript shows that for the same feedback parameters the edge states can vanish if using voltage bias far above the Fermi level. Similar reasoning applies for the heterogeneities appearing along the edge states. For all these reasons we can affirm that feedback loop instabilities do not play any significant role in our measurements.

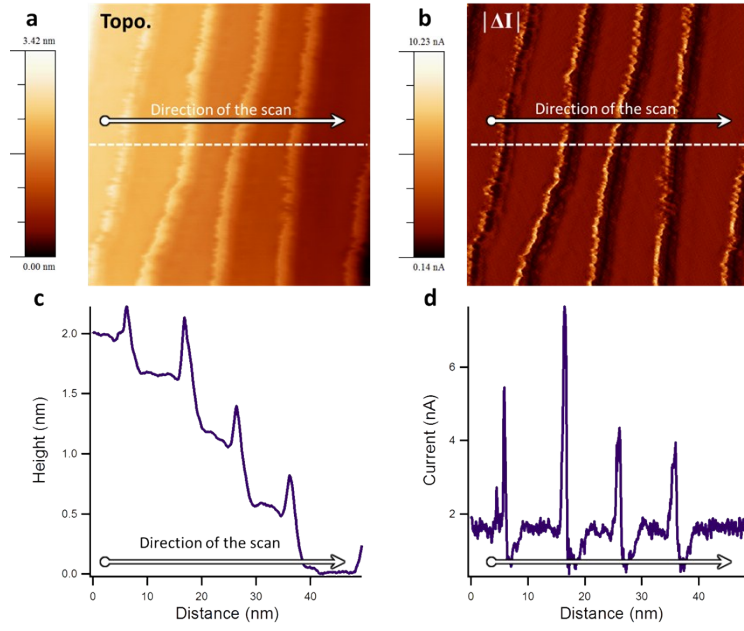


Figure Supp. 4: **a)** $50 \times 50 \text{ nm}^2$, -10 mV , 2 nA topography STM image corresponding to Fig. 2a. The direction of scan is shown by an arrow. **b)** Simultaneously obtained current error map. **c)** Topographic profile obtained along the white dashed line marked in (a) where the tip retraction due to the presence of edge states appears in every step. **d)** Current profile obtained along the white dashed line marked in (b). The 2 nA setpoint is the baseline. The sharp current spikes appear on the edge states.

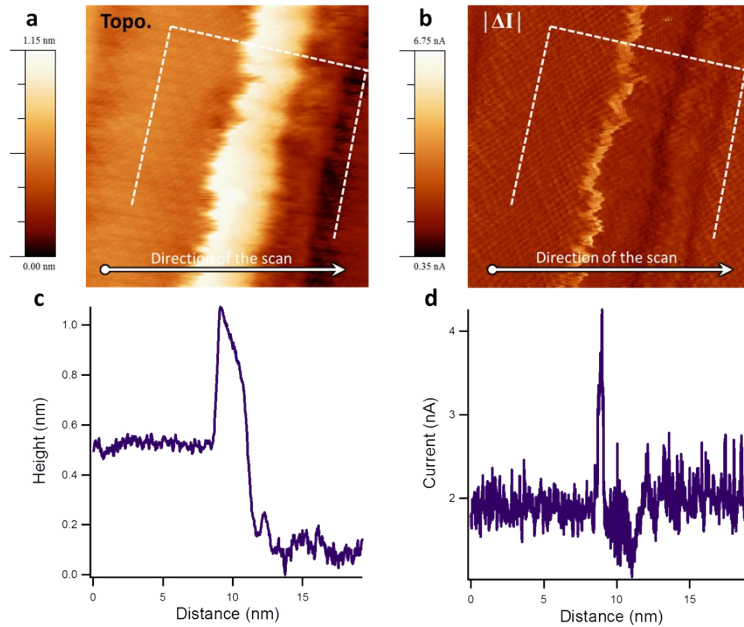


Figure Supp. 5: **a)** $10 \times 10 \text{ nm}^2$, -10 mV , 2 nA topography STM image corresponding to Fig. 2b. The direction of scan is shown by an arrow. **b)** Simultaneously obtained current error map. **c)** Topographic profile obtained along the white dashed line marked in (a) where the tip retraction due to the presence of edge states appears as a protrusion. **d)** Current profile obtained along the white dashed line marked in (b). The 2 nA setpoint is the baseline. The sharp current spikes appear on the edge state.

In order to further test any possible effect of the feedback circuit on our measurements we present additional data of a region where different angles and step-heights coexist. The STM topography presented in Fig. Supp. 6 a has been obtained using the same feedback parameters than for the data presented in Fig. 2 and 4 in the main text. The second terrace from the left presents a discontinuity across its full width at an angle of approximately 60° respect the edges of the stripes. The discontinuity runs parallel to one of the graphene high-symmetry crystallographic directions indicating that the resulting graphene edge is, in first approximation, a pure zigzag edge. In Fig. Supp. 6 b we present the simultaneously obtained current error map. We have measured (see profile in Fig. Supp. 6) and marked accordingly the height difference between terraces ($a_0 = 2.27 \text{ \AA}$). In these images, graphene edges finishing on top of single, double, and triple monoatomic Pt steps coexists. Fig. Supp. 6 c we have marked the regions of enhanced conductivity in orange on top of the topographic image. These are the regions where the edge state is stronger. The edge states obtained using this tunneling parameters form puddles along the edges of the stripes leaving segments of several nanometers with normal conductance in between. As one can notice, these regions are completely uncorrelated with the height difference between terraces, indicating that feedback effects do not play any significant role in our measurements. Very interestingly, the edge states are very strong on the zigzag edge formed in the single-Pt-slab-high step (marked within the pointed circle in Fig. Supp. 6 b), in agreement with theoretical results. The protrusion in the topographic profile related to this edge state has been marked with a red arrow in the profile presented in Fig. Supp. 6d.

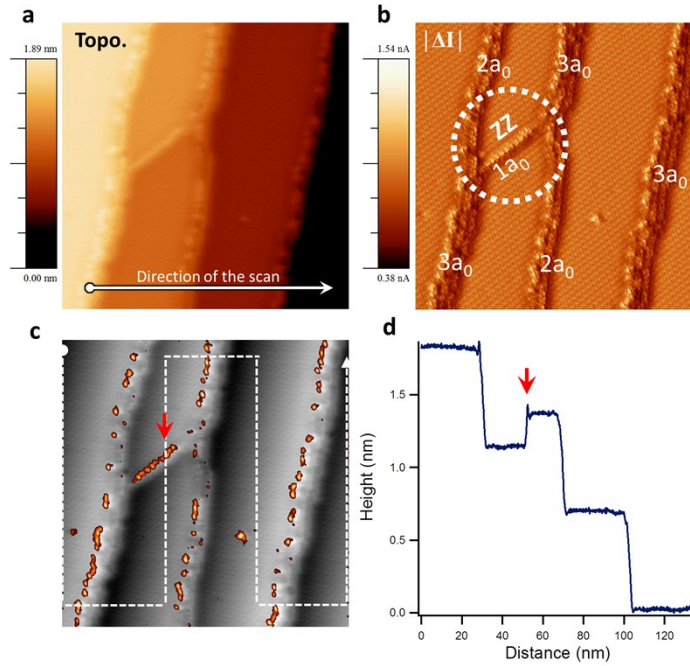


Fig. Supp. 6. a. STM topography obtained using the same feedback parameters as the ones used for obtaining the images presented in the main text ($30 \times 30 \text{ nm}^2$, $I_{\text{tunnel}} = 1 \text{ nA}$, $V_{\text{bias}} = 0.25 \text{ V}$). **b.** Current error map obtained simultaneously. **c.** STM image where the regions of enhanced conductivity are highlighted in orange. **d.** Profile obtained along the line marked in “c” where difference step heights appear. The protrusion related to the edge state of the zigzag region marked in “b” is highlighted by a red arrow.

Supplementary references:

1. M. S. José et al., *The SIESTA method for ab initio order- N materials simulation. Journal of Physics: Condensed Matter* **14**, 2745 (2002).
2. H. Santos, A. Ayuela, L. Chico, E. Artacho, *van der Waals interaction in magnetic bilayer graphene nanoribbons. Physical Review B* **85**, 245430 (2012).
3. W. Jaskólski, A. Ayuela, M. Pelc, H. Santos, L. Chico, *Edge states and flat bands in graphene nanoribbons with arbitrary geometries. Physical Review B* **83**, 235424 (2011).
4. Y.-W. Son, M. L. Cohen, S. G. Louie, *Energy gaps in graphene nanoribbons. Physical review letters* **97**, 216803 (2006).
5. C. J. Chen, *Introduction to Scanning Tunneling Microscopy, Oxford Series in Optical and Imaging Sciences, Oxford University Press*, 258-266, (1993)